Magnetic control over the topology of supramolecular rod networks

Vincent Marichez[a], Akihiro Sato[a], Peter Dunne[a], Jorge Leira-Iglesias[a], Georges J.M. Formon[a], Michaela K. Schicho[a], Isja de Feijter[b], Pascal Hébraud[c], Matthieu Bailleul[c], Pol Besenius[d], M. Venkatesan[e], J.M.D. Coey[e], E.W. Meijer[b], and Thomas M. Hermans*[a]

Abstract: Understanding and controlling supramolecular polymerization are of fundamental importance to create advanced materials and devices. Many stimuli have been explored in the past decades, but magnetic fields and field gradients have received little attention. This is because magnets do not provide enough magnetic energy to overcome thermal noise at the single molecule level. Here we show that significant changes in network topology of Gd^{3+}-decorated supramolecular polymer rods can nevertheless be observed using magnetic fields of order 1 T at room temperature. The structure of the rod networks is influenced during a slow diffusive process over a timescale of hours by the anisotropy of the demagnetizing field. Our approach opens opportunities to control and tune structure formation of many supramolecular and coordination polymers using a variety of rare earth or other paramagnetic ions.

Supramolecular polymers consist of monomers held together by reversible non-covalent interactions, and have been extensively studied in the past decades.[1] Their properties are commonly controlled by external stimuli[2], such as temperature[1], enzymes[3–5], mechanical forces[6,7], light[8–10], pH[11–13] and redox potential[14,15]. In addition, strong electric[16], magnetic,[17] or flow-fields[18,19] have been used to control the growth and orientation of supramolecular polymers. In contrast to colloidal systems where weak magnetic fields can guide assembly of ferrimagnetic nanocrystals,[20] large 10–30 T fields are typically needed to observe any effects on paramagnets at the molecular scale.

In recent years, however, several studies have reported that magnetic fields < 2 T can significantly change the assembly of molecules decorated with chelated paramagnetic ions. Specifically, Polarz *et al.*, used a C_{10}-DOTA surfactant chelating Dy^{3+}, which formed mm-size self-assembled dumbbells that could be aligned using the stray field of $Nd_2Fe_{14}B$ magnets (< 1 T).[21] Yue *et al.,* were able to orient tetrabromoferrate-modified cylindrical block-copolymer phases using just ~0.35 T.[22] Furthermore, Schefer et al., showed that polysaccharides chelated with ferric ions can stiffen 1.5-fold in a 1.1 T magnetic field. These results appear surprising considering the magnetic energies involved. In a uniform 1 T field; the magnetic energy, $U_m = -\frac{1}{2} mB$, of a single paramagnetic Gd^{3+} ion at room temperature, is $-3 \cdot 10^{-25}$ J[23], four orders of magnitude smaller than the thermal energy at room temperature $E_T = k_B T = 4 \cdot 10^{-21}$ J.

Here, we show that magnetic fields of 1 - 2 T can change the topology of supramolecular networks, which we quantify by measuring their fractal dimension. The effect is attributed to an anisotropic magnetic term in the Gibbs free energy. Specifically, we use a well-studied C_3-symmetrical benzene-1,3,5-tricarboxamide (BTA) derivative containing three 1,4,7,10-tetraazacyclododecane-N,N',N'',N'''-tetraacetic acid (DOTA) groups (Fig. 1b), which as previously shown self-assembles into rods of ~6 nm in diameter and lengths of hundreds of nm depending on the total concentration (see K_1 in Fig. 1a).[24,25] The rods assemble further into supramolecular networks (see K_2 in Fig. 1a), which as we will show in the current work, respond to magnetic fields if paramagnetic Gd^{3+} is chelated. For diamagnetic Y(III)-DOTA-BTA no changes are observed (see below).

Light scattering provides a detailed insight into the different structures and networks in aqueous solution. Figure 1c shows the measured polarized electric field autocorrelation functions $g^{(1)}_{VV}(q,t)$ at a scattering wavevector q = 0.0288 nm^{-1}, which are well represented by a distribution of relaxation times $G(\tau)$ obtained from the inverse Laplace transformation.[26]

Two distinct relaxation processes **P1** and **P2** were found (shown as solid lines underneath the correlation functions in the figure). **P1** is a fast process and **P2** is a slow one, both having q^2-dependence. That is, both processes are diffusive and their hydrodynamic radii R_H can be calculated from the diffusion constant $D_H = \Gamma \cdot q^{-2}$ (where Γ is the decay constant), using the Stokes–Einstein equation $R_H = k_B T / 6\pi\eta D_H$ (where η is the dynamic viscosity).

In figure 1d we can see that Gd(III)-DOTA-BTA forms rods with a diameter of 6 nm in agreement with our prior studies[24,25]. We can therefore convert the values of R_H of the individual rods (**P1**) by fixing the diameter and fitting rod lengths using the Tirado model[27]. This analysis leads to a rod length of ~245 nm for Gd(III)-DOTA-BTA and ~120 nm for Y(III)-DOTA-BTA (see Table 1).

Since we are dealing with rods in **P1** and networks of rods in **P2**, we tried to obtain VH (Vertical-Horizontal) polarized electric field autocorrelation functions $g^{(1)}_{VH}(q,t)$, which unfortunately were unresolved for both, even though for **P1** of Gd(III)-DOTA-BTA the $qL > 5$ [28]. Nonetheless, static light scattering intensities of both Y(III)-DOTA-BTA **P2** and Gd(III)-DOTA-BTA **P2** follow a $R(q) \propto q^{-d_F}$ power law (see Fig. 2a), allowing for the characterization of the network topology using the fractal dimension d_F (where the the lower limit of $d_F = 1$ describes a line, and the upper limit $d_F = 3$ a sphere).[29]

[a] Dr. V. Marichez, Dr. A. Sato, Dr. P. Dunne, Dr. J. Leira-Iglesias, G.J.M. Formon, M.K. Schicho, Prof. Dr. T.M. Hermans
Université de Strasbourg, CNRS, UMR7140, Strasbourg (France)
E-mail: hermans@unistra.fr
[b] Dr. I. de Feijter, Prof. Dr. E.W. Meijer
Laboratory of Macromolecular and Organic Chemistry
Eindhoven University of Technology
P.O. Box 513, 5600 MB Eindhoven (The Netherlands)
[c] Dr. P. Hébraud, Dr. M. Bailleul
Institut de Physique et Chimie des Materiaux de Strasbourg,
UMR 7504 CNRS-Université de Strasbourg
23 rue du Loess, 67034 Strasbourg (France)
[d] Prof. Dr. P. Besenius
Department of Chemistry
Johannes Gutenberg-University Mainz
Duesbergweg 10–14, 55128 Mainz (Germany)
[e] Dr. M. Venkatesan, Prof. Dr. J.M.D. Coey
Physics Department
Trinity College, Dublin 2 (Ireland)

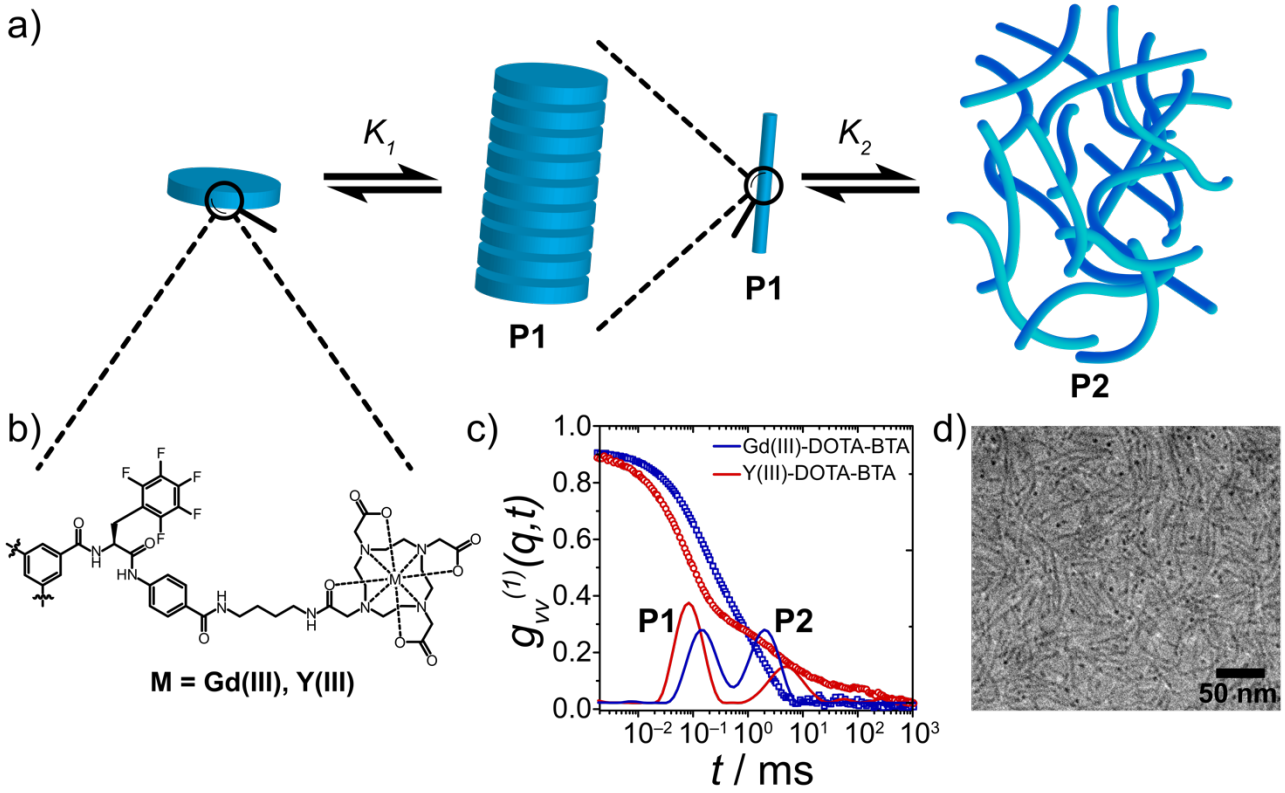

Figure 1. The formation and analysis of networks P2, consisting of supramolecular rods P1. a) Scheme depicting equilibria (K_1 and K_2) that take place during self-assembly of Gd(III)-DOTA-BTA and how the magnetic Gibbs free energies (ΔG_m) compare to thermal fluctuations at 2 T. For Y(III)-DOTA-BTA the assembly process is similar, but not affected by the applied magnetic field (not shown). b) Molecular structure of Gd(III)-DOTA-BTA and Y(III)-DOTA-BTA. Only 1 of three arms is shown for clarity. c) Polarized field correlation function $g_{VV}^{(1)}(q,t)$ at 100 µM concentration in 100 mM citrate buffer at pH 6 measured at q = 0.0288 nm^{-1}, shown by the hollow symbols. The solid lines show the corresponding distribution of relaxation times $G(\tau)$ at this wavevector, showing **P1** and **P2**. d) Cryo-transmission electron microscopy image of the rods and rod networks formed by Gd(III)-DOTA-BTA at 100 µM in 100 mM Citrate (pH = 6). The scale bar is 50 nm.

Table 1. Results from light scattering experiments. Hydrodynamic radii R_H of diffusive processes **P1** (one-dimensional rods) and **P2** (rod networks) extracted from dynamic light scattering data and the respective rod lengths estimated for **P1** according to a model by Tirado[27].

Species	R_H (**P1**) / nm	Rod length (from **P1**) / nm	R_H (**P2**) / nm
Gd(III)-DOTA-BTA	30.5 ± 4.5	245 (calc.)	348.2 ± 69
Y(III)-DOTA-BTA	17.9 ± 1.5	120 (calc.)	503.7 ± 169.6

In the absence of a magnetic field we find d_F of **P2** to be 1.7 ± 0.2 which is in agreement with a network of rods present in solution.[30,31] In addition, we performed box-counting analysis of the cryo-TEM images (see Fig. 1d and SI) of Gd(III)-DOTA-BTA leading to a d_F of 1.77–1.85, depending on the choice of threshold for converting to binary information (see SI). We are confident that process **P2** is associated with the network topology of rods of Gd(III)-DOTA-BTA.

In the experiments that follow we use d_F to quantify the rod-like network *topology*, and the Rayleigh ratio $R(q)$ to determine the approximate *mass* contained in the network. The value of $R(q)$ is derived from the static light scattering intensity, by correcting for the refractive index and subtraction of background scattering.

Practically, a light scattering cuvette was placed between the pole pieces of an electromagnet for 1 h, then analyzed by light scattering (~1 h) without field, and replaced in the magnetic field. This cycle was repeated 6–7 times (12–14 h in total). In Fig. 2b one can see that $R(q)$ for **P2** of Gd(III)-DOTA-BTA increases gradually over time, and reaches a plateau after 10–12 h that is 20% (1 T) or 35% (2 T) higher than the original value. The fractal dimension d_F changes from 1.7 ± 0.2 to 2.2 ± 0.2 (1 T) or 2.6 ± 0.2 (2 T) within the first hour and then remains constant for the rest of the experiment (see Fig. S1 in the SI). This implies that the increased magnetic field leads to increasingly dense network structures, ending up at 2 T with randomly branched clusters[32–34]. **P1** (open symbols, Fig. 2b) is unaffected by the magnetic field as explained below. If the sample is not exposed to the magnetic field, the value of $R(q)$ for **P2** remains constant (see grey dashed box in Fig. 2b). Likewise, if the chelated ion is weakly diamagnetic as in Y(III)-DOTA-BTA, no change is observed. We can therefore conclude that changes in the network topology are only observed when both paramagnetic Gd^{3+} ions and the magnetic field are present.

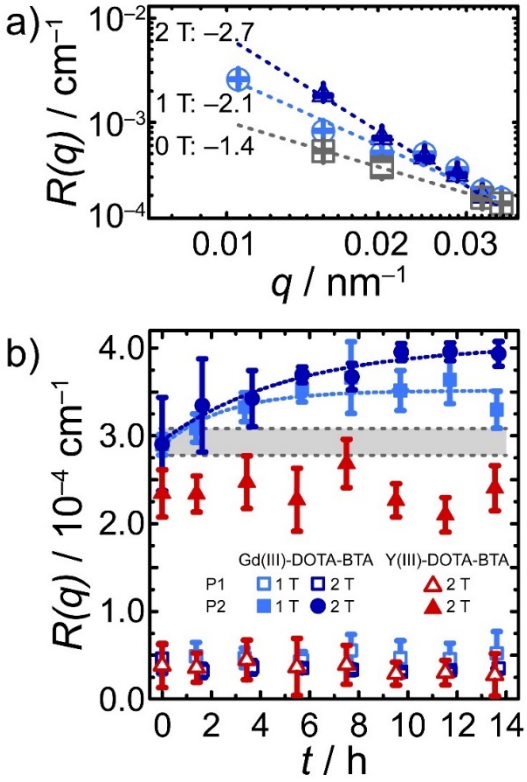

Figure 2. Quantification of rod network topologies upon exposure to magnetic fields. a) Rayleigh ratio *R(q)*, corrected scattered intensity, as a function of wavevector *q* at normal conditions (0 T) and with 1 T and 2 T applied magnetic field. The slopes of the curves give the fractal dimension of **P2** for the different magnetic fields applied. Error bars are standard deviations calculated over 5 measurements. b) Variation of Rayleigh ratio *R(q) at q* = 0.0288 nm^{-1} with time for both processes, **P1** and **P2**, denoted by hollow and filled symbols respectively. Gd(III)-DOTA-BTA is represented by circles and squares, and Y(III)-DOTA-BTA by triangles. For Y(III)-DOTA-BTA, in red, only the 2 T data is shown. The gray area delimited by pointed lines represents the control for Gd(III)-DOTA-BTA under no magnetic field (mean and standard deviation). Error bars show standard deviations over 50 measurements.

As mentioned in the introduction, the magnetic energy per ion is generally very much smaller than $k_B T$. We therefore checked for interactions between the paramagnetic ions by measuring the susceptibility versus temperature in a SQUID (superconducting quantum interference device) magnetometer. The data (Fig. 3a) show a Curie–Weiss behaviour with a very small negative paramagnetic Curie temperature of –0.7 K. Antiferromagnetic coupling between the Gd^{3+} ions in the supramolecular rods is therefore negligible, as is the crystal field interaction for Gd^{3+}, which explained alignment in the Dy^{3+} compound [21]. We also subjected samples to a constant 5 T field for up to 12 h while monitoring the magnetic susceptibility. For Gd(III)-DOTA-BTA, it decreased by ~2% with respect to the original value χ_0 on a timescale commensurate with that found in the light scattering experiments (Fig. 3b). No changes are observed in the case of Y(III)-DOTA-BTA or a buffer solution (Fig. 3b).

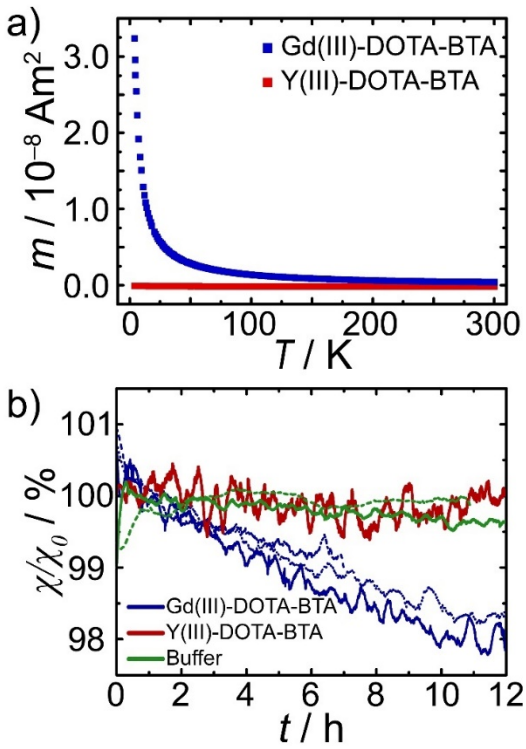

Figure 3. Magnetic characterization of supramolecular rods and networks. a) Temperature-dependent magnetization curve of Gd(III) and Y(III)-DOTA-BTA in powder form, black and red respectively. *m* represents the magnetization of the sample in A m^2. Gd(III)-DOTA-BTA shows a weak antiferromagnetic coupling –0.7 K while the Y(III) containing molecule showed no paramagnetism. b) Room-temperature time-dependent magnetization of Gd(III) and Y(III)-DOTA-BTA (blue and red lines respectively) in solution and buffer (in green). The samples were place in the SQUID under 5 T magnetic field and their magnetization was measured over the course of 12 h. The solid and dotted lines represent different runs.

To evaluate the magnetic influence in comparison to the thermal energy, the magnetic energy of a single paramagnetic monomer can be estimated using a Curie-law dependence by:[23]

$$U_{m,1} = -\frac{1}{2} m\, B = \frac{3}{2}\frac{m_{eff}^2\, B}{3\, k_B T}\, B = \frac{m_{eff}^2\, B^2}{2\, k_B T} \qquad (1)$$

Where m is the magnetic moment induced by the field B at temperature *T*, m_{eff} is the effective atomic paramagnetic moment in Am^2 (given in units of Bohr magneton μ_B). We can define a critical length L_c of the supramolecular rod, where the magnetic energy of the object exceeds the thermal energy ($|U_m| \geq k_B T$):

$$L_c = \frac{d\, k_B T}{U_{m,1}} = 2\, d \left(\frac{k_B T}{m_{eff}\, B}\right)^2 \qquad (2)$$

Here d is the π–π stacking distance of 0.35 nm between the monomers in the rod that each contain three Gd^{3+} ions.[35] The critical length and supramolecular magnetic energy for different paramagnetic ions was calculated (Table 2, and Table S4). In addition, a more detailed model considering the exact positioning of Gd^{3+} ions within the supramolecular rods, and dipole-dipole interactions, was in quantitative agreement (see SI). Overall, this shows that the magnetic energy is smaller than $k_B T$ for **P1** it can be much larger than $k_B T$ for **P2**, since the aggregates consist of a large number of entangled rods.

Table 2. Magnetic energies of assemblies and critical length for different paramagnetic ions at B = 2 T and T = 298 K. Gd^{3+} is used in the current work.

Ion	m_{eff}[23] (μ_B)	$U_{m,1}$ (J.mol^{-1}monomer^{-1})	L_c (nm)
Nd^{3+}	3.4	-0.29	2980
Gd^{3+}	8.9	-1.99	435
Tb^{3+}	9.8	-2.42	359
Dy^{3+}	10.6	-2.83	307
Ho^{3+}	10.4	-2.73	318

Let us now consider how the magnetic energy affects the network structure. Under normal conditions the distribution of **P1** and **P2** species is governed by an equilibrium constant, K_2 as seen in Fig. 1a:

$$K_2 = e^{-\frac{\Delta G_0 + \Delta G_m}{RT}}$$

where ΔG_0 is the Gibbs free energy at 298 K and 0 T. The additional term, ΔG_m, is a magnetic Gibbs free energy induced by the magnetic field, and is defined as $\Delta G_m = U_{m,rod}/2$[23] for each rod **P1** (i.e., $U_{m,rod}$ = $U_{m,1}$ x 700 monomers for Gd(III)-DOTA-BTA) added to or removed from the rod network **P2**. This is of order –0.7 kJ·mol^{-1} at 2 T, but does not influence the equilibrium constant as this energy is the same, to first order, for any spatial distribution of the Gd^{3+} ions. However, there is a small correction due to shape anisotropy:[23]

$$K_s = \frac{1}{4}\,\mu_0\,M_s^2\,(1 - 3N)$$

where N is the shape-dependent demagnetizing factor ($N = 0$ for an axially magnetized long rod), M_s is the saturation magnetization that depends on distribution of the magnetized material and μ_0 is the vacuum permeability. For the rods, $M_s = 600\ \mathrm{Am^{-1}}$. The maximum anisotropy energy is therefore $0.11\ \mathrm{Jm^{-3}}$. A sample volume of at least $k_BT/K_s = 36 \cdot 10^{-21}\ \mathrm{m^3}$ is therefore needed to overcome thermal energy. The necessary volume includes some thousands of rods since a single rod is ~$4 \cdot 10^{-24}\ \mathrm{m^3}$. This explains our experimental findings that magnetic field effects are only observed at the network level.

In conclusion, we have shown pronounced changes in the network topology of supramolecular polymer rods containing paramagnetic ions upon applying magnetic fields of 1–2 T, accessible without resorting to cryogenic superconductor magnets. The magnetic energies involved are insignificant at the single rod level; they become significant only at the network scale.

In general, supramolecular polymers provide a versatile platform to assemble many magnetic ions into larger substructures and make them susceptible to the fields from modern permanent magnets or Halbach arrays. Our approach therefore opens opportunities to control and guide structure formation of supramolecular and coordination polymers using rare earth or paramagnetic ions, in order to tune collective effects in magnetic field-responsive dynamic materials.

Acknowledgements

VM, AS, JLI, and TMH would like to acknowledge the funding from ANR-10-LABX-0026 CSC. GJMF received funding from Ministère de l'Education Nationale de l'Enseignement supérieur et de la Recherche. EWM acknowledges funding of the Dutch Ministry of Education, Culture and Science (Gravitation program 024.001.035). PD and TMH acknowledge the support of the Labex NIE 11-LABX-0058_NIE within the Investissement d'Avenir program ANR-10-IDEX-0002-02, the support of the University of Strasbourg Institute for Advanced Studies (USIAS) Fellowship. PD acknowledges support from SALTYSPIN ANR-17-CE09-0005.

Keywords: supramolecular polymer • rare earth ion • magnet • magnetic equilibrium

[1] T. Aida, E. W. Meijer, *Isr. J. Chem.* **2020**, *60*, 33–47.
[2] T. Aida, E. W. Meijer, S. I. Stupp, *Science* **2012**, *335*, 813–817.
[3] A. R. Hirst, S. Roy, M. Arora, A. K. Das, N. Hodson, P. Murray, S. Marshall, N. Javid, J. Sefcik, J. Boekhoven, J. H. Van Esch, S. Santabarbara, N. T. Hunt, R. V. Ulijn, *Nature Chemistry* **2010**, *2*, 1089–1094.
[4] M. J. Webber, C. J. Newcomb, S. I. Stupp, *Soft Matter* **2011**, *7*, 9665–9672.
[5] A. Sorrenti, J. Leira-Iglesias, A. Sato, T. M. Hermans, *Nature Communications* **2017**, *8*, 15899.
[6] J. M. A. Carnall, C. A. Waudby, A. M. Belenguer, M. C. A. Stuart, J. J. P. Peyralans, S. Otto, *Science* **2010**, *327*, 1502–1507.
[7] J. T. Van Herpt, M. C. A. Stuart, W. R. Browne, B. L. Feringa, *Langmuir* **2013**, *29*, 8763–8767.
[8] B. Adhikari, Y. Yamada, M. Yamauchi, K. Wakita, X. Lin, K. Aratsu, T. Ohba, T. Karatsu, M. J. Hollamby, N. Shimizu, H. Takagi, R. Haruki, S. Adachi, S. Yagai, *Nature Communications* **2017**, *8*, ncomms15254.
[9] R. Iwaura, T. Shimizu, *Angewandte Chemie - International Edition* **2006**, *45*, 4601–4604.
[10] L. Li, H. Jiang, B. W. Messmore, S. R. Bull, S. I. Stupp, *Angew. Chem. Int. Ed.* **2007**, *46*, 5873–5876.
[11] J. Zhang, R. Hao, L. Huang, J. Yao, X. Chen, Z. Shao, *Chemical Communications* **2011**, *47*, 10296–10298.
[12] H. Frisch, J. P. Unsleber, D. Lüdeker, M. Peterlechner, G. Brunklaus, M. Waller, P. Besenius, *Angew. Chem. Int. Ed.* **2013**, *52*, 10097–10101.
[13] T. J. Moyer, J. A. Finbloom, F. Chen, D. J. Toft, V. L. Cryns, S. I. Stupp, *J. Am. Chem. Soc.* **2014**, *136*, 14746–14752.
[14] E. Ohta, H. Sato, S. Ando, A. Kosaka, T. Fukushima, D. Hashizume, M. Yamasaki, K. Hasegawa, A. Muraoka, H. Ushiyama, K. Yamashita, T. Aida, *Nature Chemistry* **2010**, *3*, 68–73.
[15] J. Leira-Iglesias, A. Sorrenti, A. Sato, P. A. Dunne, T. M. Hermans, *Chemical Communications* **2016**, *52*, 9009–9012.
[16] P. Van Der Schoot, M. E. Cates, *The Journal of Chemical Physics* **1994**, *101*, 5040–5046.
[17] T. J. Drye, M. E. Cates, *The Journal of Chemical Physics* **1993**, *98*, 9790–9797.
[18] R. Bruinsma, W. M. Gelbart, A. Ben-Shaul, *The Journal of Chemical Physics* **1992**, *96*, 7710–7727.
[19] M. S. Turner, M. E. Cates, *Journal Phys: Condensed Matter* **1992**, *4*, 3719–3741.
[20] G. Singh, H. Chan, A. Baskin, E. Gelman, N. Repnin, P. Král, R. Klajn, *Science* **2014**, *345*, 1149–1153.
[21] S. Polarz, C. Bährle, S. Landsmann, A. Klaiber, *Angewandte Chemie - International Edition* **2013**, *52*, 13665–13670.
[22] B. Yue, X. Jin, P. Zhao, M. Zhu, L. Zhu, **2019**, *1804572*, 1–7.
[23] J. M. D. Coey, *Magnetism and Magnetic Materials*, Cambridge University Press, Cambridge, UK, **2009**.
[24] P. Besenius, G. Portale, P. H. H. Bomans, H. M. Janssen, A. R. A. Palmans, E. W. Meijer, *PNAS* **2010**, *107*, 17888–17893.
[25] I. De Feijter, P. Besenius, L. Albertazzi, E. W. Meijer, A. R. A. Palmans, I. K. Voets, *Soft Matter* **2013**, *9*, 10025–10030.
[26] S. W. Provencher, *Computer Physics Communications* **1982**, *27*, 213–227.
[27] M. M. Tirado, C. L. Martínez, J. G. de la Torre, *J. Chem. Phys.* **1984**, *81*, 2047–2052.
[28] R. Pecora, *The Journal of Chemical Physics* **1968**, *48*, 4126–4128.
[29] J. A. Raper, R. Amal, *Particle & Particle Systems Characterization* **1993**, *10*, 239–245.
[30] A. Mohraz, D. B. Moler, R. M. Ziff, M. J. Solomon, *Physical Review Letters* **2004**, *92*, 1555031–1555034.
[31] L. A. Hough, M. F. Islam, B. Hammouda, A. G. Yodh, P. A. Heiney, *Nano Letters* **2006**, *6*, 313–317.
[32] D. W. Schaefer, *Science* **1989**, *243*, 1023–1027.
[33] D. W. Schaefer, J. M. Brown, D. P. Anderson, J. Zhao, K. Chokalingam, D. Tomlin, J. Ilavsky, in *Journal of Applied Crystallography*, **2003**, pp. 553–557.

[34] B. J. Bauer, E. K. Hobbie, M. L. Becker, *Macromolecules* **2006**, *39*, 2637–2642.
[35] J. W. Steed, J. L. Atwood, *Supramolecular Chemistry*, John Wiley & Sons, Ltd, Chichester, UK, **2009**.